EXO-200 results and cosmogenic backgrounds

V A Belov (for the EXO-200 collaboration)

SSC RF ITEP of NRC "KI", B. Cheremushkinskaya, 25, Moscow, 117218, Russia

E-mail: belov@itep.ru

Abstract. Status update and recent results from the double beta decay search experiment EXO-200 are presented. Detector is a liquid xenon TPC with charge and light readout located underground in low-background laboratory at 1600 m.w.e. depth. It contains 175 kg of xenon with 80.6% abundance of ^{136}Xe, which acts as both the decaying nucleus and detection medium. Detector showed good performance and achieved remarkable results. The detector has demonstrated excellent energy resolution and background rejection capabilities and has set a lower limit on the $0\nu\beta\beta$-decay half-life of 1.1×10^{25} years at 90% C.L. in early 2014. The EXO-200 collaboration has since published several papers on experimental backgrounds and searches for rare or exotic processes. After a two-year data interruption, EXO-200 is now back online with significant hardware improvements, including a radon reduction air system and a front end electronics upgrade for better energy resolution.

1. Introduction

Nuclear beta decay is a known process in which a nucleon decays, releasing an electron (positron) and an electron antineutrino (or neutrino). For some even-even nuclei, this single beta decay is forbidden or highly suppressed and it becomes possible to observe double beta decay, when two nucleons decay simultaneously. The half-lives for $\beta\beta$ decay are very long (typically of order $10^{18} - 10^{21}$ years) since it is a second-order weak process. This decay has been observed in a number of isotopes. Xenon was one of the last unseen. The hypothetical neutrinoless ($0\nu\beta\beta$) decay mode can only occur if neutrino is a massive Majorana particle [1]. This decay may be mediated by the exchange of a Majorana neutrino or by other new particles. The $0\nu\beta\beta$ decay rate is related to the square of an effective Majorana neutrino mass $\langle m \rangle_{\beta\beta}$ by the product of phase space and a nuclear matrix element squared. Direct kinematic measurements restrict the neutrino mass scale to be below ~2 eV [2-3], leading to $0\nu\beta\beta$ half-lives beyond 10^{24} yr.

The exceedingly long half-lives of interest for $0\nu\beta\beta$ decay require large detectors using isotopic enriched sources, radio-clean construction techniques and the ability to actively reject remaining backgrounds. The $0\nu\beta\beta$ decay results in a discrete electron sum energy distribution centered at the Q-value ($Q_{\beta\beta}$). The allowed, yet also rare, two neutrino double beta ($2\nu\beta\beta$) decay is characterized by a continuous sum energy spectrum ending at $Q_{\beta\beta}$. The sum energy of decay electrons allows discrimination between the two modes. The $2\nu\beta\beta$ decay has been observed in many isotopes [4] and, recently, in ^{136}Xe with the EXO-200 detector [5], later confirmed in [6]. Several experiments are running to test $0\nu\beta\beta$ decay discovery on ^{76}Ge but it is important to test this also with different nucleus like ^{136}Xe.

2. Detector

EXO-200 was designed to be a state of the art double beta decay experiment and, at the same time, a technology test bed for a future, larger detector. In order to take advantage of event topology, xenon self-shielding, and the possibility of purifying a noble element before and during its use, EXO-200 uses the xenon as both source and detector in a single homogeneous volume (for a detailed description see [7]). In order to minimize the surface-to-volume ratio while maintaining a practical geometry, the detector is a double TPC, having the shape of a square cylinder. Of the 200 kg of enriched xenon available, 175 kg are in liquid phase, and 110 kg are in the active volume of the detector. Isotope composition is 80.6% of the ^{136}Xe and the remaining 19.4% is ^{134}Xe. A cutaway view of the TPC is shown in figure 1. Gas system allows to recirculate and purify xenon continuously.

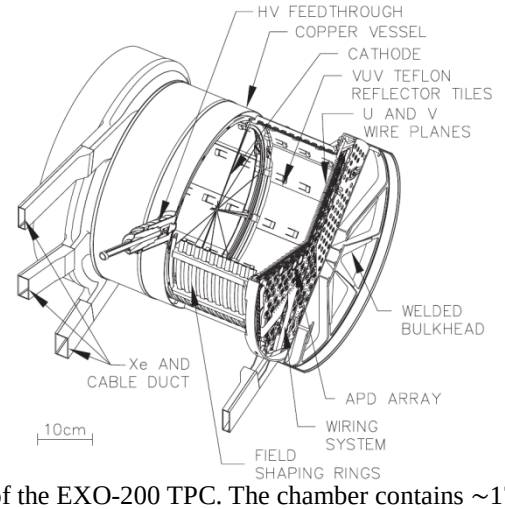

Figure 1. Drawing of the EXO-200 TPC. The chamber contains ~175 kg of liquid xenon.

Charged particles produce energy depositions in the TPC. This energy through ionization and excitation of xenon atoms produce both ionization electrons and scintillation photons. In EXO-200 both the ionization and the scintillation signals are recorded. The cylindrical TPC is divided into two symmetric volumes separated by a cathode grid. Ionization electrons drift along applied electric field from center towards ends of the TPC. Each end of the TPC holds grid of 38 charge induction (V) and 38 charge collection (U) wire triplets. The U and V wire grids, oriented at 60◦ from each other, provide planar information for charge depositions. At each end of the TPC there are ~250 Large Area Avalanche PhotoDiodes (LAAPDs) that record the 178 nm xenon scintillation light and make 41% of area coverage. The TPC configuration allows for three-dimensional topological and temporal reconstruction of individual energy depositions. This ability is essential for discriminating $\beta\beta$ decays from residual backgrounds dominated by gammas.

At least 50 cm of HFE-7000 fluid plus 10 cm of copper and 25 cm of low-activity lead shield the TPC from external radioactivity. The clean room module housing the TPC is surrounded on four sides by 50 mm thick plastic-scintillator cosmic-ray veto panels, which are (96.35 ± 0.11)% efficient. To reduce cosmogenic and radioactive background EXO-200 is located at a depth of 1624^{+22}_{-21} m.w.e. at the WIPP salt mine in New Mexico, USA.

3. Reconstruction

Offline event reconstruction proceeds in three stages: signal finding, parameter estimation, and clustering. Charge signals on the U wires and scintillation signals on the two LAAPD planes are found using a matched filter technique. The filter yields time estimates for both ionization and scintillation channels. The time information from the U wires is used to search for induction signals in V wire waveforms. Candidate U wire signals are fit to template waveforms modeling the measured transfer functions so that the signal amplitudes can be extracted for energy estimation. Amplitudes are corrected, channel-by-channel, for electronic gains determined from radioactive source calibration.

U wire and V wire signals are then combined into charge clusters using timing information from the fits, and associated with the nearest (earlier in time) summed scintillation signal. Matching signals at two wire planes (U and V) provides planar coordinates for each ionization cluster. Three-dimensional position sensitivity is achieved by using the difference in the arrival time between the ionization and scintillation signals to calculate the electron drift time. Events with one charge cluster per one scintillation cluster are called single site events (SS) and events with many charge clusters per one scintillation cluster are called multiple site events (MS). The ability of the TPC to identify SS and MS interactions is used to separate β and $\beta\beta$ decays in the bulk xenon from multiple site γ interactions. The standoff distance, defined as the shortest distance between and the edge of the TPC or the cathode, are calculated. Majority of β-like signal events are SS events uniformly distributed inside the detector. On the other hand, the γ-like backgrounds are mostly MS events close to the detector constructions.

Each cluster energy is corrected for position-dependent charge losses due to finite xenon purity and for the shielding grid inefficiency of the V wire plane. This procedure, introducing the only time-dependent correction, yields a reconstructed ionization energy and three dimensional position information for each charge cluster. An efficiency loss is incurred by events for which 3D reconstruction is not possible as these are rejected from this analysis. The LAAPD signal are passed through a dedicated algorithm called 'denoising' [8] that takes into account pulse size from waveform fit, pulse size expected from charge clusters, measured noise in this channel and combines this into total scintillation energy. It is corrected for variations of gain and spatial light collection efficiency within the TPC. An interpolation of the 2615 keV gammas SS full absorption peak scintillation signal is used to construct the correction function.

As first discussed in [9] anti-correlation of charge vs scintillation signal can be used to reduce energy reconstruction error. The 2D SS and MS energy spectra are independently rotated and projected onto a new (1D) energy variable in such a way as to minimize the width of the 2615 keV line. Positional information about event is used in form of standoff distance (SD) that is a minimal distance from any charge cluster to any piece of detector construction except cathode. Obtained binned distributions over energy and SD for both SS and MS events are fitted using maximum likelihood to a probability density functions (PDF) of various sources and backgrounds. Such PDFs are created with Montre-Carlo simulation software based on GEANT4 [10] libraries.

EXO-200 experiment utilizes various techniques to measure and track detector performance. Calibration runs are performed daily. It includes charge and light injection as well as in-situ measurements with gamma-ray sources. Individual wire and APD gains are measured and electronics stability and linearity is monitored with dedicated runs. Compact gamma sources are used for final energy calibration. The energy calibration function that converts the rotated energy estimator into keV is almost linear but has a small quadratic term. The energy resolution is found to be $\sigma/E = 1.53\%$ (1.65%) for SS (MS) spectra at $Q_{\beta\beta}$, dominated by the noise and broadening terms.

4. Results

EXO-200 began low-background data taking in June 2011. The detector successfully operated for two and half years before underground accidents at WIPP temporarily halted operations. Using the first two years of data, the collaboration published the first $2\nu\beta\beta$ observation for ^{136}Xe in [5] and later improved the measurement with $T_{1/2} = 2.165 \pm 0.016(\text{stat}) \pm 0.059(\text{syst}) \times 10^{21}$ years [11]. In 2014, EXO-200 set a sensitive lower limit on ^{136}Xe $0\nu\beta\beta$ $T_{1/2}$ at 1.1×10^{25} years with 90% C.L. [12]. The global fit of the low-background spectra predicts a background rate of 1.7×10^{-3} kg^{-1}yr^{-1}keV^{-1} in the region of interest. EXO-200 had published 8 papers during last two years [13-15], including an investigation of radioactivity-induced backgrounds [16], deep study of cosmogenic backgrounds [17] and a search for ^{136}Xe $2\nu\beta\beta$ decay into the first excited state (0_1^+) of ^{136}Ba [18].

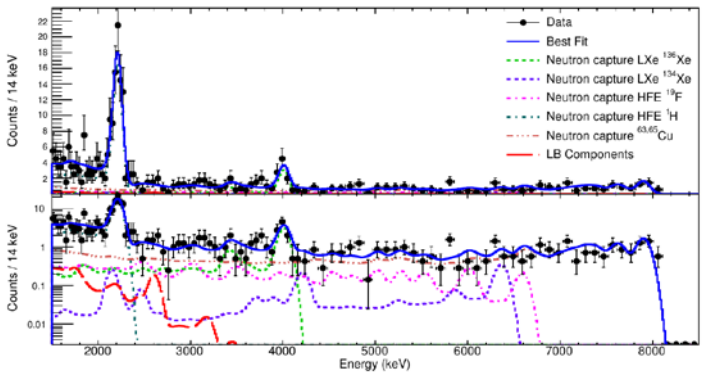

Figure 2. MS spectrum and the veto-tagged data fit. The different panels show results on a linear and logarithmic scale.

5. Cosmogenic backgrounds

Being an ultra-pure experiment, EXO-200 took great care in selecting low radioactivity materials and constructed the detector in clean environment. Studies were done to better understand the location and strength of various background sources and selective backgrounds investigated is discussed here; for more information and details on various radioactivity-induced backgrounds, please consult [16].

A special care must be taken upon neutron activation of materials. Neutrons are more penetrating particles than gamma, and they also produce much smaller signals due to quenching. Another origin of problems comes from cosmic muons. Yet easily tagged they are almost unstoppable, at least for a human-made shield. Passage of muons produces not only a prompt signals but also delayed signals from neutrons capture and activated isotopes decay. For an ultra-pure experiment this may lead to an irreducible background if neutrons are captured on core detector materials or the detecting media itself. In case of our xenon the most dangerous thing is neutron capture on ^{136}Xe. Resulting ^{137}Xe β decays and has a half-life of 229.1 ± 0.8 s with a Q-value of 4173 ± 7 keV.

A dedicated study of this question was performed. We simulated muons in EXO-200 using FLUKA and GEANT4. In order to verify our simulation we compared neutron-capture γ events in simulation and our detector. Events are within 10 μs – 5 ms time window after active veto signal (see figure 2). Obtained rates agree for both FLUKA and GEANT4 simulation. A big study was made to check all of activation isotopes indicated from simulation. Results show that only ^{137}Xe put a significant impact on low-background spectra and predicted rate is consistent with results of $0\nu\beta\beta$ analysis [17].

6. Recent upgrades and current detector performance

During a two-year hiatus in data taking we prepared some upgrades for EXO-200 detector. One long-awaiting thing is a deradonator for the air gap between the copper cryostat and the lead shield wall. The deradonator consists of two stainless columns filled with charcoal. While air from the air gap is drawn into one column, the other column undergoes desorption under vacuum, providing capability to purge 30 cfm of air with reduced radon content constantly. Preliminary measurement shows that the radon level of the air gap has been reduced by more than a factor of 10 since the deradonator installation.

Another promising change is electronics upgrade, that allowed to decrease a coherent noise significantly. For example in APD channels noise was reduced by a factor of 2.5 while signal increased by ~5%. We also managed to increase cathode voltage to 12kV, which increased drift field strength.

By applying denoising algorithm [8], reducing APD coherent noise with new electronics, and increasing drift field strength, energy resolution in the region of interest has been improved from an average of 1.58% to 1.28% (see figure 3). Current source calibration data shows better shape agreement with MC simulations. Purity in the detector has increased to about 3.5 ms. EXO-200 low background data taking began on April 29, 2016 and is expected to take data until 2018. Sensitivity studies indicate that

EXO-200 can reach a *0νββ* decay half-life sensitivity of 5.7×10^{25} yr, after Phase-II operation (see figure 4). Although EXO-200 is unlikely to pass the recent ^{136}Xe *0νββ* decay limit set by KamLAND-Zen [19], the EXO-200 result will provide an important check for the KamLAND-Zen result with different systematic uncertainties and demonstrate the capabilities of LXe TPC for future tonne-scale detectors.

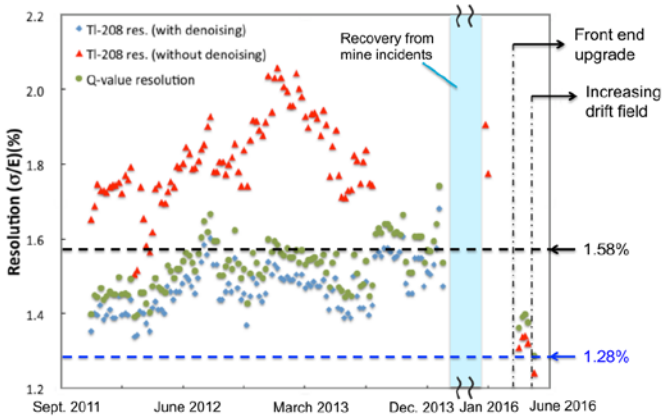

Figure 3. Shown is resolution for SS events at the ^{208}Tl full-absorption peak and at the 0νββ Q-value versus time. The horizontal dashed line shows the effective energy resolution for Phase-I data set (1.58%, black) and for Phase-II data (1.28%, blue).

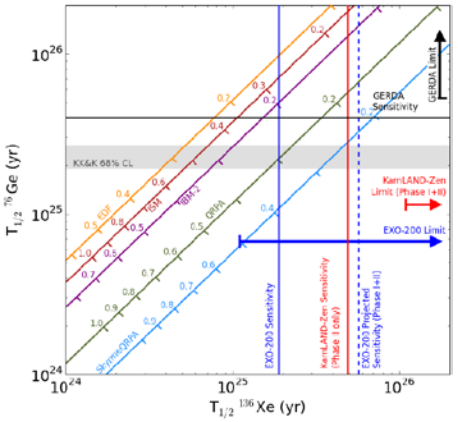

Figure 4. Comparison of 0νββ half-lives results between ^{76}Ge and ^{136}Xe with different matrix element calculations. The most recent results from GERDA [16], EXO-200 and KamLAND-Zen are shown. The dotted blue line shows projected combined Phase-I and Phase-II sensitivity for EXO-200.

Acknoledgements

EXO-200 is supported by DoE and NSF in the United States, NSERC in Canada, SNF in Switzerland, NRF in Korea and RFBR in Russia. This research used resources of the National Energy Research Scientific Computing Center (NERSC). The collaboration gratefully acknowledges the WIPP for the hospitality.

References

[1] Schechter J and Valle J W F 1982 *Phys. Rev.* D **25**(11) 2951
[2] Aseev V N *et al.* 2011 *Phys. Rev.* D **84**(11) 112003
[3] Kraus Ch *et al.* 2005 *Eur. Phys. J.* C **40**(4) 447
[4] Barabash A S 2010 *Phys. Rev.* C **81** 035501
[5] Ackerman N *et al.* 2011 *Phys. Rev. Lett.* **107**(21) 212501
[6] Gando A *et al.* 2012 *Phys. Rev.* C **85**(4) 045504
[7] Auger M *et al.* 2012 *JINST* **7** P05010
[8] Davis C G *et al.* 2016 *JINST* **11**(07) P07015
[9] Conti E *et al.* 2003 *Phys. Rev.* B **68**(5) 054201
[10] Agostinelli S *et al.* 2003 *Nucl. Inst. Meth.* A **506**(3) 250
[11] Albert J B *et al.* 2014 *Phys. Rev.* C **89**(1) 015502
[12] Albert J B *et al.* 2014 *Nature* **510** 229
[13] Albert J B *et al.* 2016 *Phys. Rev.* D **93**(7) 072001
[14] Albert J B *et al.* 2016 *J. Cosmol. Astropart. Phys.* **2016**(04) 029
[15] Albert J B *et al.* 2015 *Phys. Rev.* C **92** 045504
[16] Albert J B *et al.* 2014 *Phys. Rev.* D **90** 092004
[17] Albert J B *et al.* 2015 *Phys. Rev.* C **92**(1) 015503
[18] Albert J B *et al.* 2016 *Phys. Rev.* C **93**(3) 035501
[19] Gando A *et al.* 2016 *Phys. Rev. Lett.* **117** 082503